Prediction of the Thermal Parameters of a High-Temperature Metallurgical Reactor Using Inverse Heat Transfer

Mohamed Hafid, Marcel Lacroix

Abstract—This study presents an inverse analysis for predicting the thermal conductivities and the heat flux of a high-temperature metallurgical reactor simultaneously. Once these thermal parameters are predicted, the time-varying thickness of the protective phase-change bank that covers the inside surface of the brick walls of a metallurgical reactor can be calculated. The enthalpy method is used to solve the melting/solidification process of the protective bank. The inverse model rests on the Levenberg-Marquardt Method (LMM) combined with the Broyden method (BM). A statistical analysis for the thermal parameter estimation is carried out. The effect of the position of the temperature sensors, total number of measurements and measurement noise on the accuracy of inverse predictions is investigated. Recommendations are made concerning the location of temperature sensors.

Keywords—Inverse heat transfer, phase change, metallurgical reactor, Levenberg–Marquardt method, Broyden method, bank thickness.

I. INTRODUCTION

HIGH-temperature metallurgical reactor such aluminum-electrolysis-cells (Fig. 1) are used for material processing that requires high powers and elevated temperature. Their applications are in the production of aluminum and the smelting of materials such as steel, copper and nickel calcine.

A fascinating solid/liquid phase change phenomenon that arises in these metallurgical reactors is the formation of a bank that covers the inside surface of the refractory brick wall. The presence of this bank is extremely important. It protects the inner lining of the refractory brick wall from the highly corrosive slag. On the other hand, too thick a bank is detrimental to the industrial production as the volume available for smelting is reduced. Therefore, keeping a bank of optimal thickness is crucial for the safe and profitable operation of the metallurgical reactor.

Due to the hostile conditions that prevail inside these reactors, it is however very difficult and risky to measure the bank thickness using probes submerged into the corrosive slag (The standard method). Additionally, the transient formation of the bank depends on the boundary conditions, the power input, and the thermos physical properties of the slag. Consequently, predicting the transient formation of the

Hafid M. and Lacroix M. are with the Department of Mechanical Engineering, Université de Sherbrooke, 2500 Blvd. de l'Université, Sherbrooke (Québec) J1K 2R1, Canada (Phone: (873) 888-7768, (819)821-8000; e-mail: mohamed.hafid@usherbrooke.ca, Marcel.Lacroix@uSherbrooke.ca).

protective bank inside high-temperature metallurgical reactor is a challenging problem. To address this problem, an inverse heat transfer procedure is proposed. The prediction of the bank formation with inverse heat transfer methods has been the subject of few investigations in the past. These methods rest on the conjugate gradient method [1]-[4], the Kalman filter method [5]-[9] and the LMM [10]. In all of these studies, the focus was on the inverse prediction of the time-varying heat flux at $(x=L_{Brick} + L_{PCM})$ using the transient temperature measurements, or heat flux measurements, taken at a specified location inside the refractory brick wall (Fig. 2). Once the heat flux had been predicted, the time-varying bank thickness $E(t)$ was calculated using the direct model.

The objective of the present study is to extend these previous studies by predicting simultaneously several unknown quantities of interest that is the time-varying heat flux $q''(t)$, the thermal conductivity in liquid PCM, the thermal conductivity in solid PCM and the thermal conductivity of refractory brick wall (Fig. 4).

II. PROBLEM STATEMENT AND MATHEMATICAL MODEL (DIRECT MODEL)

The one-dimensional phase-change problem for a High-temperature Metallurgical Reactor is depicted in Fig. 2. The inner lining of the brick wall $(x=L_{Brick})$ is coated with a protective bank whose thickness is $E(t)$. $E(t)$ represents the position of the solidification front for the Phase Change Material (PCM). The outer surface of the brick wall $(x=0)$ is cooled with an air stream. The outside temperature is T_∞ and the convective heat transfer coefficient h_∞.

At $(x= L_{Brick} + L_{PCM})$, a time-varying heat flux $q''(t)$ is imposed over the time interval $t\epsilon[0, 400000\ (s)]$.

The proposed mathematical model rests on the following assumptions [1], [3], [4], [6], [7]:

- The temperature gradients in the x direction are much larger than those in the other directions. As a result, a one-dimensional analysis can be applied.
- The heat transfer inside the liquid phase of the PCM is conduction dominated [11].
- The thermal properties of the phase change material (PCM) are temperature independent.
- The phase change problem is non-isothermal. The melting process is depicted by three zones: a solid phase, a mushy zone and a liquid phase.
- The thermal contact resistance between the refractory brick wall and the PCM is neglected.

World Academy of Science, Engineering and Technology
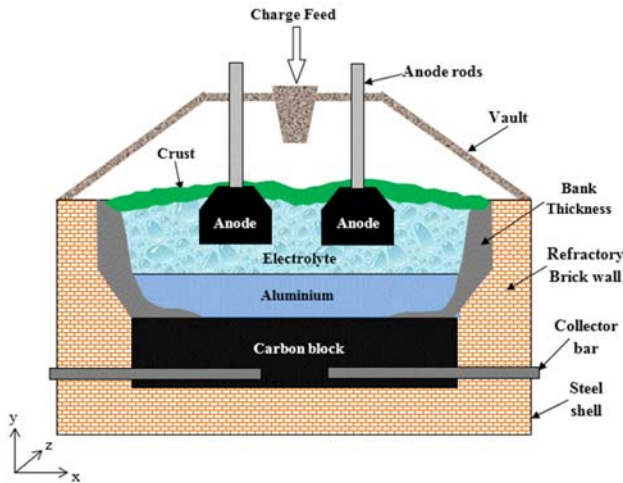International Journal of Mechanical and Mechatronics Engineering
Vol:10, No:6, 2016

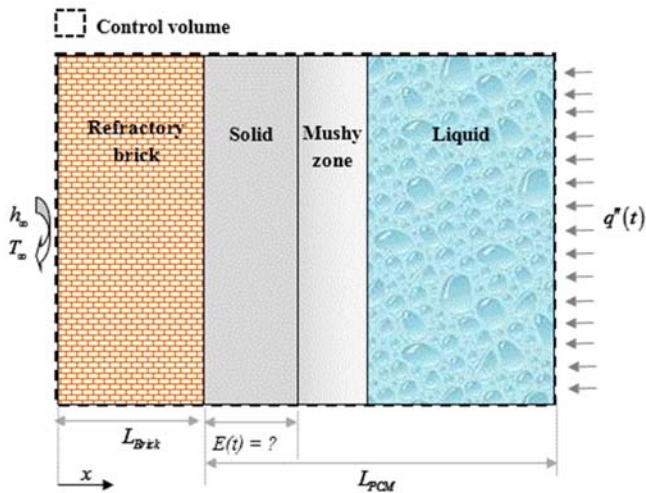Fig. 1 Cross view of a typical high-temperature metallurgical reactor

Fig. 2 Schematic of a one-dimensional phase-change problem for a high-temperature metallurgical reactor

Based on these assumptions, the governing heat diffusion equation is expressed as:

$$\rho C_p \frac{\partial T}{\partial t} = \frac{\partial}{\partial x}\left(k \frac{\partial T}{\partial x}\right) - \delta H \frac{\partial f}{\partial t} \qquad (1)$$

where δH and f are the enthalpy and the liquid fraction, respectively. The enthalpy δH is defined as

$$\delta H = \rho(C_{p,liquid} - C_{p,solid})T + \rho \lambda \qquad (2)$$

The liquid fraction f varies linearly between the solidus T_{sol} and the liquidus T_{liq} in the following manner:

$$f = F(T) \begin{cases} 0 & T \leq T_{sol} & (Solid \text{ region}) \\ \dfrac{T - T_{sol}}{T_{liq} - T_{sol}} & T_{sol} \leq T \leq T_{liq} & (Mushy \text{ region}) \\ 1 & T \geq T_{liq} & (Liquid \text{ region}) \end{cases} \qquad (3)$$

At each time-step, the liquid fraction f is updated iteratively in the following manner [12]:

$$f^{k+1} \approx f^k + \left(\frac{dF}{dT}\right)^k \left(T^{k+1} - F^{-1}\left(f^k\right)\right) \qquad (4)$$

F^{-1} is the inverse function of F. The boundary conditions at the left and right sides of Fig. 2 are:

$$\begin{cases} \left(-k \dfrac{\partial T}{\partial x}\right)_{x=0} = \overline{h}\left(T(0,t) - T_\infty\right) \\ \left(-k \dfrac{\partial T}{\partial x}\right)_{x=L_{Brick}+L_{PCM}} = q''(t) \end{cases} \qquad (5)$$

Equations (1)-(5) are solved numerically using a Finite-Volume Method (FVM). The scheme adopted for the time discretization is implicit. The resulting set of algebraic equations is solved using the Tri-Diagonal-Matrix-Algorithm (TDMA) [13].

The mathematical model was first validated using the one-dimensional test case for the solidification of the binary Al–4.5% Cu alloy reported in [12], [14]. In this example, a Dirichlet boundary condition of $T=573$ (K) is assumed at the boundary $x=L_{Brick}$ (Fig. 2). The width of the PCM layer is set equal to $L_{PCM}=0,5$ (m) and the initial temperature is fixed at $T_{in}=969$ (K).

Fig. 3 shows the predicted time-varying phase front are in excellent agreement with the source-based numerical method [12] and the semi-analytical heat balance integral method [14].

Next, the direct model was implemented for the entire metallurgical reactor i.e. the refractory brick wall and the PCM (Fig. 2). The operating thermal conditions of the metallurgical reactor are similar to those reported in [6], [7]. The brick wall is set equal to $L_{Brick}=0,1$ (m) and the PCM layer (solid, mushy, and liquid) is set equal to $L_{PCM}=0,1$ (m) (Fig. 2). The surrounding temperature is set equal to $T_\infty=300$ (K) and the outside average heat transfer coefficient is fixed at $h_\infty=15$ $(W/m^2 K)$.

The time-varying heat flux $q''(t)$ at $(x=L_{Brick}+L_{PCM})$ is given by

$$q''(t) = Q_0 + Q_1 * \sin^2\left(\frac{3\pi.t}{t_{max}}\right) \qquad (6)$$

It is also assumed that the PCM thermal conductivity in the solid and liquid phases is temperature independent. The thermo-physical properties of the metallurgical reactor (brick wall and PCM) are provided in Table I [6], [7].
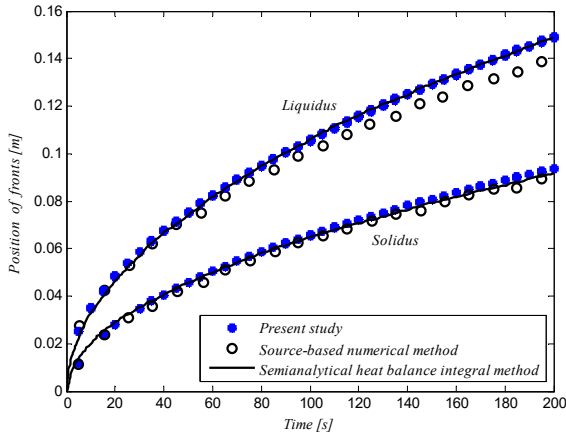
World Academy of Science, Engineering and Technology
International Journal of Mechanical and Mechatronics Engineering
Vol:10, No:6, 2016

Fig. 3 Solidification of a binary Al–4,5%-Cu alloy

TABLE I
THERMO-PHYSICAL PROPERTIES OF THE BRICK WALL AND PCM

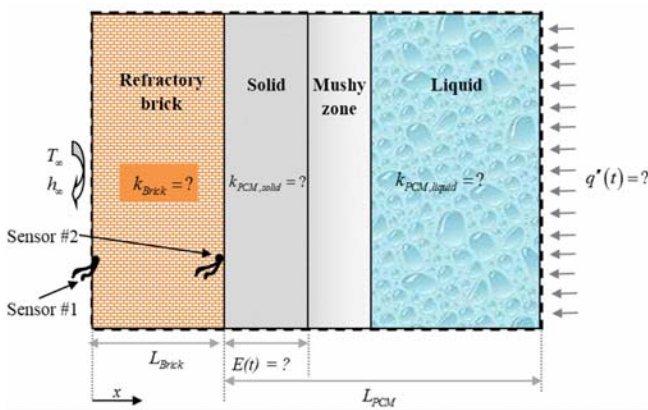| Parameter	Value	Unit
k_{BRICK}	16,8	(W/m K)
$C_{p,BRICK}$	875	(J/kg K)
ρ_{BRICK}	2600	(kg/m³)
$k_{PCM,solid}$	1	(W/m K)
$k_{PCM,liquid}$	10	(W/m K)
$C_{p,PCM,solid}$	1800	(J/kg K)
$C_{p,PCM,liquid}$	1800	(J/kg K)
ρ_{PCM}	2100	(kg/m³)
λ_{PCM}	5,1 x 10⁵	(J/kg)
T_{sol}	1213	(K)
T_{liq}	1233	(K)

Fig. 4 The inverse problem: k_{Brick}, $k_{PCM,solid}$, $k_{PCM,liquid}$ and $q''(t)$ are
unknown. They are determined from temperatures taken by probes
(sensor #1 or sensor #2) embedded into the brick wall

III. THE INVERSE MODEL

In the direct model presented above, all the physical and the geometrical properties are known. For the inverse model, it is assumed that the parameters of: the heat flux $q''(t)$, the thermal conductivity of the brick wall k_{Brick}, the thermal conductivity

in the solid PCM $k_{PCM,solid}$ and in the liquid PCM $k_{PCM,liquid}$ are unknown (Fig. 4).

The objective of the inverse model is to determine the unknown thermal parameters for $q''(t)$ and thermal conductivities, i.e. $\vec{P} = \left[Q_0; Q_1; k_{brick}; k_{PCM,solid}; k_{PCM,liquid} \right]$.

The additional information required for the estimation of these thermal parameters, is the time-varying temperature recorded by a sensor (thermocouple) embedded into the refractory brick wall Fig. 4. Once the thermal parameters are estimated, the bank thickness $E(t)$ is determined from the direct model presented above.

The estimation of the thermal parameters from measured can be constructed as a problem of minimization of the least square norm $\Psi\left(\vec{P}\right)$:

$$\Psi\left(\vec{P}\right) = \sum_{i=1}^{I} \left[Y(t_i) - \hat{T}(t_i, \vec{P}) \right]^2 \qquad (7)$$

$P = (P_1, P_2,...P_5)$ is the set of the unknown thermal parameters. I is the total number of measurements. $Y(t_i)$ are the temperatures measured by the sensor. In the present study, these temperatures are 'generated' from the solution of the direct model. $\hat{T}(t_i, \vec{P})$ are the estimated temperatures from the inverse model.

The Levenberg–Marquardt Method was adopted for minimizing the least square norm, (7). The incremental value of the unknown parameter ΔP, is expressed as:

$$\Delta\vec{P} = \left[\left(\vec{J}^k\right)^T \vec{J}^k + \mu^k \vec{\Omega}^k \right]^{-1} \left(\vec{J}^k\right)^T \left(\vec{Y} - \vec{T}(\vec{P}^k)\right) \qquad (8)$$

μ^k is a positive damping parameter. More details on the choice and the update of this parameter are provided in [15]. $\vec{\Omega}^k$ is the diagonal matrix of $\left(\vec{J}^k\right)^T \vec{J}^k$. The superscript 'T' denotes the transpose of the matrix. The superscripts "⁻" and "⃗" refer to the matrix and vector notation, respectively. $\vec{J}^k$ is the Jacobian matrix. It is given by:

$$\vec{J}\left(\vec{P}\right) = \begin{pmatrix} \dfrac{\partial T_1}{\partial P_1} & \dfrac{\partial T_1}{\partial P_2} & \dfrac{\partial T_1}{\partial P_3} & \dfrac{\partial T_1}{\partial P_4} & \dfrac{\partial T_1}{\partial P_5} \\ \dfrac{\partial T_2}{\partial P_1} & \dfrac{\partial T_2}{\partial P_2} & \dfrac{\partial T_2}{\partial P_3} & \dfrac{\partial T_2}{\partial P_4} & \dfrac{\partial T_2}{\partial P_5} \\ \vdots & \vdots & \vdots & \vdots & \vdots \\ \dfrac{\partial T_I}{\partial P_1} & \dfrac{\partial T_I}{\partial P_2} & \dfrac{\partial T_I}{\partial P_3} & \dfrac{\partial T_I}{\partial P_4} & \dfrac{\partial T_I}{\partial P_5} \end{pmatrix} \qquad (9)$$

The Jacobian matrix (the sensitivity matrix) plays a very important role in the estimation of the parameters. There are several approaches for computing the sensitivity coefficients $\partial T_i/\partial P_j$ [16]. In this study, the sensitivity coefficients are approximated with a finite difference:

World Academy of Science, Engineering and Technology
International Journal of Mechanical and Mechatronics Engineering
Vol:10, No:6, 2016

$$J_{ij} = \frac{\partial \hat{T}_i}{\partial P_j} \cong \frac{\hat{T}\left(t_i; P_1, ..., P_j + (\delta P_j), ... P_N\right) - \hat{T}\left(t_i; P_1, ..., P_j - (\delta P_j), ... P_N\right)}{2(\delta P_j)} \quad (10)$$

The parameter perturbation (δP_j) is set to $\xi(1 + |P_j|)$. ξ is a small number. The subscripts i and j represent the time and the parameter respectively.

In order to diminish the computational effort, the Jacobian matrix is updated using the Broyden update expression [17].

For the first iteration, for every 2*N iterations and for iterations that satisfy $\Psi(P + \Delta P) > \Psi(P)$, the sensitivity coefficients $\partial T_i / \partial P_j$ of the Jacobian matrix are estimated with (10). For every other iteration, the Jacobian matrix is updated using the Broyden expression:

$$J_k = J_{k-1} + \frac{\left(\left(\hat{T}_k - \hat{T}_{k-1}\right) - J_{k-1} \Delta P_{k-1}\right) \Delta P_{k-1}^T}{\Delta P_{k-1}^T \Delta P_{k-1}} \quad (11)$$

ΔP_{k-1} is the incremental value of the unknown parameters. J_k and J_{k-1} are the Jacobian matrices at the current and previous iteration, respectively.

Convergence of the LMM is declared when one of the following criteria is satisfied

$$\begin{cases} J^T \left\| Y(t_i) - \hat{T}(t_i, \vec{P}) \right\| < \varepsilon_1 \\ \left(\frac{P^{k+1} - P^k}{P^{k+1}}\right) < \varepsilon_2 \\ \Psi\left(P^{k+1}\right) < \varepsilon_3 \end{cases} \quad (12)$$

$(\varepsilon_1; \varepsilon_2; \varepsilon_3)$ are small numbers.

The Levenberg–Marquardt computational procedure for the inverse problem is summarized as:

Step 1: Solve the direct problem (1)-(5) in order to obtain the temperature field T_{exact}.

Step 2: Compute the least square norm $\Psi(P)$ from (7).

Step 3: Compute the sensitivity coefficients according to (10) or the Broyden update expression (11).

Step 4: Compute the increment ΔP of the estimated parameters from (8).

Step 5: Solve the direct problem with the new estimate P^{k+1} in order to find $T(P^{k+1})$. Then compute $\Psi(P^{k+1})$ as defined in step 2.

Step 6: Check for convergence as defined in (12). If convergence is not achieved, go back to Step 3, update the sensitivity coefficients and $\Psi(P)$.

Once the vector of the thermal parameters has been estimated, the bank $E(t)$ is easily determined from the direct model.

IV. STATISTICAL ANALYSIS FOR PARAMETERS ESTIMATION

In order to assess the accuracy and the uniqueness of the solution and to obtain confidence intervals, a statistical analysis for parameter estimation was performed. Moreover, it was assumed that the signal temperature is contaminated with measurement errors. For distributed measurement errors with zero mean and constant variance σ^2, the standard deviation of the estimated parameters can be defined as [16]

$$\sigma_{P_j} = \sigma \sqrt{diag\left\{\left(\frac{\partial T^T}{\partial P}\right)\left(\frac{\partial T}{\partial P^T}\right)\right\}^{-1}} \quad (13)$$

Assuming a normal (or Gaussian) distribution for temperature measurement errors and 99% confidence, the bounds for the computed quantities P_j are determined as

Probability:

$$\left\{\left(\hat{P}_j - 2.576 \, \sigma_{\hat{P}_j}\right) < P_{j,exact} < \left(\hat{P}_j + 2.576 \, \sigma_{\hat{P}_j}\right)\right\} \cong 99\% \quad (14)$$

$\hat{P}_j$ are the estimated values of the unknown parameters, $P_{j,exact}$, for $(j=1...5)$, and $\sigma_{\hat{P}_j}$ are the standard deviations obtained from (13).

V. RESULTS AND DISCUSSION

The above inverse heat transfer computational procedure was employed to predict simultaneously the heat flux $q''(t)$ and the thermal conductivities (k_{Brick}, $k_{PCM,solid}$ and $k_{PCM,liquid}$) inside a high-temperature metallurgical reactor (Fig. 4). Once these parameters are estimated, the time-varying bank thickness $E(t)$ is calculated from the direct model presented in Section II.

The measured temperatures were collected with a sensor embedded into the refractory brick wall at two different locations: The first location, called 'Sensor#1', is near the outer surface of the brick wall. The second position, 'Sensor#2', is close to the molten material PCM (Fig. 4). The total number of temperature measurements I during the interval $t\epsilon[0, 400000 (s)]$ is 2000.

Note that the uniqueness and the accuracy of the inverse procedure have been thoroughly tested with noisy data and for different positions of the sensor. These results are not reported here.

For the sake of comparing the inverse predictions 'Inverse model' to the exact solution 'Direct model', three different estimation errors are defined in the following manner:

$$\text{Error}_{E(t)} = 100 \times \frac{\left|E(t_i)_{exact} - E(t_i)_{inverse}\right|}{\left|E(t_i)_{exact}\right|} \quad (15)$$

$$\text{RRMSE}_{E(t)} \% = 100 \times \sqrt{\frac{1}{I}\sum_{i=1}^{I}\left(\frac{E(t_i)_{exact} - E(t_i)_{inverse}}{E(t_i)_{exact}}\right)^2} \quad (16)$$

$$Error_P \% = 100 \times \frac{\left|P_{exact} - P_{inverse}\right|}{\left|P_{exact}\right|} \quad (17)$$

World Academy of Science, Engineering and Technology
International Journal of Mechanical and Mechatronics Engineering
Vol:10, No:6, 2016

The effect of the sensor location (Sensor#1 and Sensor#2) on the estimation of the unknown parameters is summarized in Table II. It is seen that the error on the parameters estimation is less than 0,7%. It is also observed that sensor#2 (embedded deeper into the brick wall) provides the best parameter estimation.

The convergence for the unknown thermal parameters $\vec{P} = \left[Q_0 ; \; Q_1 ; \; k_{brick} ; \; k_{PCM,solid} ; k_{PCM,liquid} \; \right]$ is plotted in Fig. 5.

TABLE II
EFFECT OF THE SENSOR POSITION

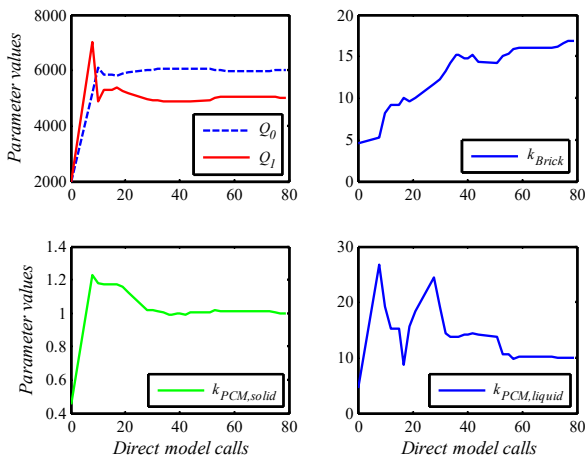|	P_{Exact}	Sensor#1		Sensor#2	
		$P_{Inverse}$	$Error_P\%$	$P_{Inverse}$	$Error_P\%$
$Q_0 (W/m^2)$	6000	5998.29	0,03	6001.84	0,03
$Q_1 (W/m^2)$	5000	5003.46	0,07	5001.17	0,02
$k_{brick} (W/m\,k)$	16.8	16.88	0,48	16.85	0,30
$k_{solid} (W/m\,k)$	1	1.00	0.00	1.00	0.00
$k_{liquid} (W/m\,k)$	10	9.93	0,70	9.99	0,10

Fig. 5 Convergence of the parameter values (Sensor#1, no noise)

The finite-difference approximation of the sensitivity coefficients, (9), requires the solution of the direct problem five times (number of unknown parameters) per iteration. As a result, the computations may quickly become prohibitive. To alleviate the computational effort, the sensitivity matrix was updated with the BM [17]. This strategy has already been applied successfully in the field of inverse heat transfer (IHTP) [18], [19]. Table III shows that the solution using the LMM combined with BM (LMM/BM) is achieved more efficiently than that with the LMM.

TABLE III
THE CONVERGENCE OF LMM AND LMM/BM

	Direct model calls	CPU time (s)
LMM	90	4468,92
LMM/BM	79	3502,98

All simulations were conducted with the Matlab software running on an Intel ® Core(TM) i5-2520M CPU @ 2,50GHz.

The effect of the temperature-sensor location on the accuracy of the predicted bank thickness $E(t)$ is depicted in

Fig. 6. For both sensors, i.e., sensor#1 and sensor#2, the $Error_{E(t)}$ on the predicted bank thickness remains less than 0.1%. The effect of the sensor location appears to be insignificant [1]. Therefore, for practical reasons, sensor#1 is recommended over sensor#2. It is indeed much safer and easier to embed a sensor near the outer surface of the refractory brick wall. This result should be of interest to the process industry.
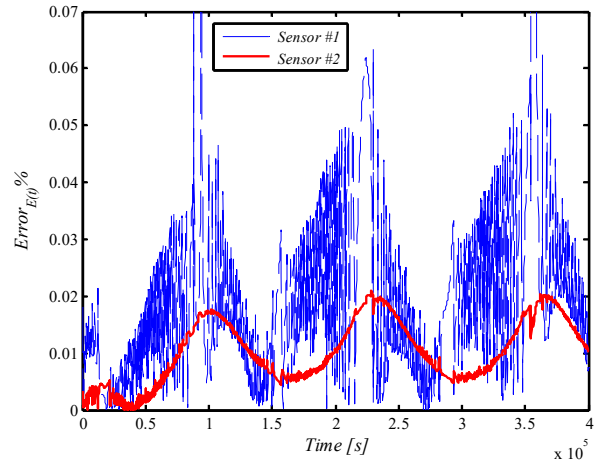

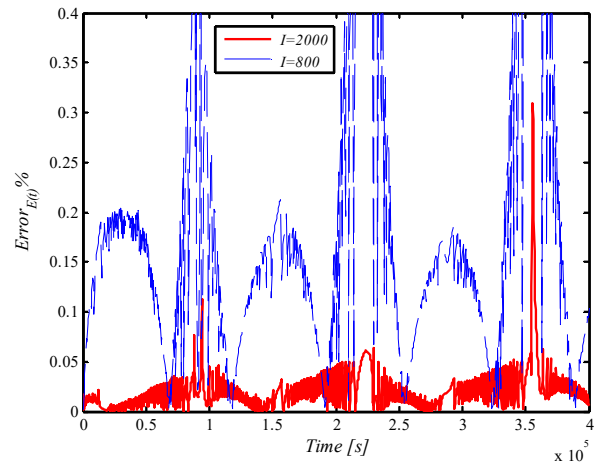Fig. 6 Effect of the sensor position on the predicted bank thickness $E(t)$

Fig. 7 Effect of the total number of measurements on the $Error_{E(t)}$

Fig. 7 shows the effect of the total number of measurements I on the accuracy of the predictions for the bank thickness. Accuracy improves when the total number of measurements is raised from $I=800$ to $I=2000$. The higher the total number of measurements, the better.

In order to mimic temperature measurement errors, a random error noise $\vec{\omega}_i$ is added to the exact temperature $\vec{T}_{exact}$ generated by the direct model in the following manner:

$$\vec{T}(t_i) = \vec{T}_{exact}(t_i) + \sigma\vec{\omega}_i \tag{18}$$

World Academy of Science, Engineering and Technology
International Journal of Mechanical and Mechatronics Engineering
Vol:10, No:6, 2016

σ is the standard deviation of the measurement errors, which may take the value of *2% T_{max}* and *4% T_{max}*. *T_{max}* is the maximum temperature measured by the sensor.
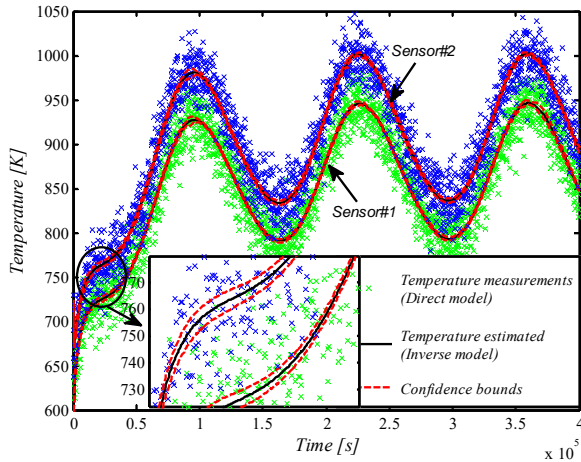

Fig. 8 Measured and inverse temperature (Sensor#1 and Sensor#2, *σ=2% T_{max}*)
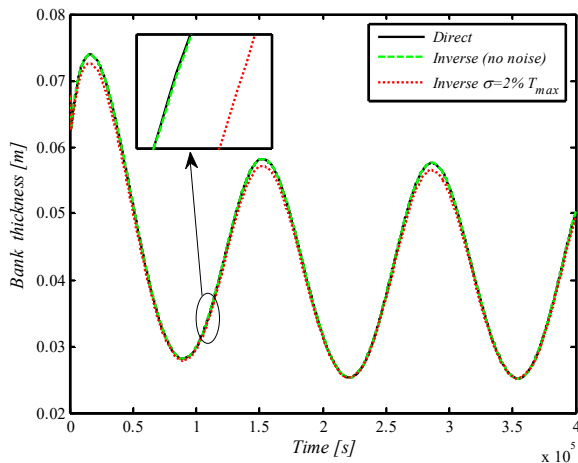

Fig. 9 Effect of the noise on the predicted bank thickness from sensor #1

Fig. 8 compares the measured temperatures provided by the direct model with *σ=2%T_{max}* to the estimated temperatures predicted by the inverse model with both sensors. The confidence intervals $\pm 2.576\ \sigma_{\hat{P}_j}$ are also shown.

Fig. 9 illustrates the effect of the noise level on the predicted bank thickness *E(t)* using sensor #1. As expected, when the noise level rises to *2%T_{max}*, the relative root-mean-square error for the bank thickness $RRMSE_{E(t)}$ increases form 0,03% to 1,43%. Nevertheless, the inverse model remains stable and accurate with experimental noise.

VI. CONCLUSION

An inverse heat transfer method was presented for predicting the time-varying thickness of the protective bank inside a high-temperature metallurgical reactor. It was shown that the inverse method may predict simultaneously the heat flux $q''(t)$, the thermal conductivity of the brick wall k_{Brick} and the thermal conductivity of the solid and liquid phases of the PCM ($k_{PCM,solid}$ and $k_{PCM,liquid}$). The proposed inverse method rests on the LMM/BM. It was shown that LMM/BM is computationally more efficiently than the LMM. The effect of the measurement noise, of the location of the temperature sensors and of the total number of measurements on the inverse predictions was investigated. Recommendations were made concerning the location of the sensor embedded into the refractory brick wall.

NOMENCLATURE

C_p	specific heat (J/kg K)
dt	time step (s)
f	liquid fraction
h	heat transfer coefficient (W/m²K)
I	total number of measurements
J	Jacobian matrix
k	thermal conductivity (W/mK)
L_{Brick}	width of the brick wall (m)
L_{PCM}	width of the PCM layer (m)
N	number of unknown parameters
$q''(t)$	heat flux (W/m²)
P	vector of unknown parameter
PCM	phase change material
$Error$	estimation errors (%)
$E(t)$	bank thickness (m)
t	time (s)
$\hat{T}$	estimated temperature (K)
x	Cartesian spatial coordinate (m)
Y	measured temperature (K)
ε	small number
μ	damping parameter
ρ	density (kg/m³)
σ	standard deviation of the measurement error
ψ	sum of squares norm
ξ	small number
δH	enthalpy (J/m3)
Δ	difference
Ω^k	diagonal matrix
λ	heat of fusion (J/kg)
ω	random number

Subscripts

0	initial value
∞	ambient
$Brick$	brick wall
$Exact$	exact solution
$E(t)$	bank thickness
liq	liquidus

World Academy of Science, Engineering and Technology
International Journal of Mechanical and Mechatronics Engineering
Vol:10, No:6, 2016

$liquid$	liquid (PCM)
$\max$	maximum
PCM	phase change material
$q^{"}(t)$	heat flux
sol	solidus
$solid$	solid (PCM)

Superscripts

k	time iteration number
T	transposed matrix
$\hat{\ }$	estimated parameter
$\rightarrow$	vector
$\leftrightarrow$	matrix.

REFERENCES

[1] O. Tadrari and M. Lacroix, Prediction of Protective Banks in High-Temperature Smelting Furnaces by Inverse Heat Transfer, Int. J. of Heat and Mass Transfer, vol. 49, no. 13–14, pp. 2180–2189, 2006.

[2] M. A. Marois, M. Désilets, and M. Lacroix, Prediction of a 2-D Solidification Front in High-Temperature Furnaces by an Inverse Analysis, Numer. Heat Transfer A, vol. 59, no. 3, pp. 151–166, 2011.

[3] M. A. Marois, M. Désilets, and M. Lacroix, Prediction of the Bank Formation in High Temperature Furnaces by a Sequential Inverse Analysis with Overlaps, Numer. Heat Transfer A, vol. 60, pp. 561–579, 2011.

[4] M. A. Marois, M. Désilets, and M. Lacroix, What is the Most Suitable Fixed Grid Solidification Method for Handling Time-Varying Inverse Stefan Problems in High Temperature Industrial Furnaces? Int. J. of Heat and Mass Transfer, vol. 55, pp. 5471–5478, 2012.

[5] C. Bertrand, M. A. Marois, M. Désilets, G. Soucy, and M. Lacroix, A combined 2D inverse predictions and experimental analysis for the bank formation internal a metallurgical reactor, Int. J. of Heat and Mass Transfer, vol. 59, pp. 58-65, 2013.

[6] M. LeBreux, M. Désilets, and M. Lacroix, Fast Inverse Prediction of Phase Change Banks in High-Temperature Furnaces with a Kalman Filter Coupled with a Recursive Least-Square Estimator, Int. J. of Heat and Mass Transfer, vol. 53, no. 23–24, pp. 5250–5260, 2010.

[7] M. LeBreux, M. Désilets, and M. Lacroix, An unscented Kalman filter inverse heat transfer method for the prediction of the ledge thickness internal high-temperature metallurgical reactors, Int. J. of Heat and Mass Transfer, vol. 57, no. 1, pp. 265-273, 2013.

[8] M. LeBreux, M. Désilets, and M. Lacroix, Control of the Ledge Thickness in High-Temperature Metallurgical Reactor using a Virtual Sensor, Inverse Problems in Sci. and Eng., vol. 20, no. 8, pp. 1215–1238, 2012.

[9] M. LeBreux, M. Désilets, and M. Lacroix, Prediction of the Time-Varying Ledge Profile internal a High-Temperature Metallurgical Reactor with an Unscented Kalman Filter-Based Virtual Sensor, Numer. Heat Transfer A, vol. 64, pp. 551-576, 2013.

[10] M. LeBreux, M. Désilets, and M. Lacroix, Is the performance of a virtual sensor employed for the prediction of the ledge thickness internal a metallurgical reactor affected by the thermal contact resistance? WIT Transactions on Eng. Sci. , Vol. 83, pp. 517-526, 2014.

[11] V. Guillaume, L. Gosselin, and M. Lacroix, an enhanced thermal conduction model for the prediction of convection dominated solid–liquid phase change, Int. J. of Heat and Mass Transfer, vol. 52, no. 7-8, pp. 1753-1760, 2009.

[12] V. R. Voller and C. R. Swaminathan, General Source-Based Method for Solidification Phase Change, Numer. Heat Transfer, vol. 19, pp. 175–189, 1991.

[13] S. V. Patankar, Numerical Heat Transfer and Fluid Flow, McGraw-Hill, New York, 1980.

[14] V. R. Voller, Development and application of a heat balance integral method for analysis of metallurgical solidification, Applied Mathematical Modelling, pp. 3-11, 1989.

[15] D. W. Marquardt, An algorithm for least-squares estimation of nonlinear parameters, J. of the Society for Industrial and Applied Mathematics, pp. 431-441, 1963.

[16] M. N. OZISIK and H. R. B. Orlande, Inverse Heat Transfer: Fundamentals and Applications, Taylor and Francis, New York, 2000.

[17] C. G. Broyden, A class of methods for solving nonlinear simultaneous equations, Mathematics of computation, pp. 577-593, 1965.

[18] B. Moghadassian, and F. Kowsary, Inverse boundary design problem of natural convection–radiation in a square enclosure, Int. J. of Thermal Sci. vol. 75, pp. 116-126, 2014.

[19] K. W. Kim, and S. W. Baek, Inverse radiation–conduction design problem in a participating concentric cylindrical medium, Int. J. of Heat and Mass Transfer, vol. 50, no. 13-14, pp. 2828-2837, 2007.